Atmospheric Research 153 (2014) 98–118

Contents lists available at ScienceDirect

Atmospheric Research

journal homepage: www.elsevier.com/locate/atmos

12 September 2012: A supercell outbreak in NE Italy?

Agostino Manzato [a,*,1], Silvio Davolio [b], Mario Marcello Miglietta [b], Arturo Pucillo [a,1], Martin Setvák [c]

[a] OSMER - Osservatorio Meteorologico Regionale dell'ARPA Friuli Venezia Giulia, Via Oberdan 18/a, I-33040 Visco (UD), Italy
[b] ISAC CNR - Institute of Atmospheric Sciences and Climate, National Research Council, Bologna–Lecce, Italy
[c] CHMI — Czech Hydrometeorological Institute, Prague, Czech Republic

ARTICLE INFO

Article history:
Received 18 December 2013
Received in revised form 16 July 2014
Accepted 16 July 2014
Available online 5 August 2014

Keywords:
Supercell
Severe storm
Doppler radar
LAM
MSG rapid scan

ABSTRACT

On 12 September 2012 a sequence of convective events hit the northeastern part of Italy and in particular the eastern part of Veneto and the plain of Friuli Venezia Giulia regions. During the day at least two events could be classified as supercells, the first one being also associated with a heavy hailfall. After a few hours, a third storm system, resembling a squall-line, although of limited dimensions, swept over the area.

This event occurred during the first Special Observing Period (SOP1) of the HyMeX project as IOP2 (Intense Observing Period) and – also for this reason – many observations managed by different institutions were collected, including Doppler radar, extra-soundings, sodar and surface stations. Moreover, EUMETSAT was conducting its first experimental 2.5-minute rapid scan with the MSG-3 satellite, with data available from early morning until 0900 UTC of the IOP2 day.

Several mesoscale models were run during the HyMeX SOP to support the field operations. A comparison between simulations of two high-resolution models (MOLOCH and WRF) is presented here and shows the capability in forecasting the intense convective activity in the area, although the exact temporal evolution of the systems was missed. Model simulations also provide useful insights concerning the mesoscale conditions conducive to the development of the convective systems.

Finally, a diagnostic tool (Corfidi and Bunkers vectors) is applied using the model wind field, in order to infer further information on the temporal evolution of the convective cells.

1. Introduction

Northeastern Italy (NEI hereafter) is a peculiar region from the point of view of severe weather, since a high frequency of thunderstorms (Cacciamani et al., 1995; Feudale et al., 2013; Isotta et al., 2013), hailstorms (Morgan, 1973; Giaiotti et al., 2003; Manzato, 2012), and other high impact events including flash floods (Borga et al., 2007; Davolio et al., 2009; Barbi et al., 2012) and bow-echo-like storms (Pucillo and Manzato, 2010) are observed. For these reasons NEI was chosen as one of the three Italian target areas of the first Special Observation Period (SOP1, 5 September–6 November 2012; Ducrocq et al., in press) of the HYdrological cycle in the Mediterranean EXperiment (HyMeX, http://www.hymex.org).

HyMeX is an international program aimed at improving the scientific knowledge of the water cycle variability in the Mediterranean basin. This is pursued through monitoring, analysis and modeling of the regional hydrological cycle. In this context, a special emphasis is given to the occurrence of heavy precipitations and floods, which often affect the Mediterranean region, considering also the associated impacts on society. Given the central position of the Italian territory in the Mediterranean basin, and its exposure to severe weather and to the consequent hydro-geological effects, the interest in improving the understanding of high impact weather events in the area is clearly evident.

During SOP1 many Intense Observation Periods (IOPs) were activated as a result of daily discussions between the HyMeX

* Corresponding author.
E-mail address: agostino.manzato@osmer.fvg.it (A. Manzato).
[1] Tel.: +39 0432 934163; fax: +39 0432934100.

http://dx.doi.org/10.1016/j.atmosres.2014.07.019
0169-8095/

Operational Centre (HOC) in Montpellier and the Italian operational center in L'Aquila, hosted by CETEMPS (Center of Excellence for the integration of remote sensing TEchniques and numerical Modelling for the Prediction of Severe weather). Decisions concerning the IOPs were taken after the analysis of the available real-time meteorological model simulations and through discussions among forecasters, including those of the involved regional operational centers (i.e. for NEI target area, SIMC — ARPA Emilia Romagna http://www.arpa.emr.it/sim, CMT ARPA Veneto http://www.arpa.veneto.it/previsioni/it/html/index.php, and OSMER — ARPA Friuli Venezia Giulia http://www.meteo.fvg.it/home.php). The specific IOP discussed in this work (IOP2, 12 September 2012) is analyzed in Kerkmann et al. (2012) and is one of the three IOPs briefly discussed in Ferretti et al. (2014), where an overview of the participation of the Italian community to the HyMeX SOP activity is provided. However, in those papers only the early morning phase of the whole event is analyzed briefly. In contrast, in the present study, all the different storms that affected NEI during the whole day are investigated in more detail.

The aim of the present study is to provide a deeper understanding of the mesoscale mechanisms responsible for the different events, using also insights from high resolution models and from very rapidly updated experimental satellite data. The critical usefulness of this innovative satellite product is clearly revealed by this specific application.

The paper is organized as follows. In Section 2 the available observation and modeling platforms, employed in the study, are described, while Section 3 provides a synoptic and mesoscale analysis of IOP2, based on observations. Section 4 discusses the modeling results, while Section 5 presents a study of the observed trajectories of the cell-centroids and of their forecast based on model winds. Lastly, conclusions are drawn in Section 6.

2. Data

2.1. In-situ instruments (stations, sounding)

The area of interest (Fig. 1, that reports all the locations quoted in this work) is monitored with a dense ground-station network. The regional meteorological office of Veneto region (CMT — ARPAV) manages about 200 meteorological surface stations, reporting data every 15 min. In Friuli Venezia Giulia (FVG) region there are about 250 surface stations, partly managed by the regional Civil Protection Agency and partly by the regional meteorological office (OSMER — ARPA FVG). The time sampling rate of these stations ranges from 5 min in most of the about 50 stations managed by OSMER — ARPA FVG to

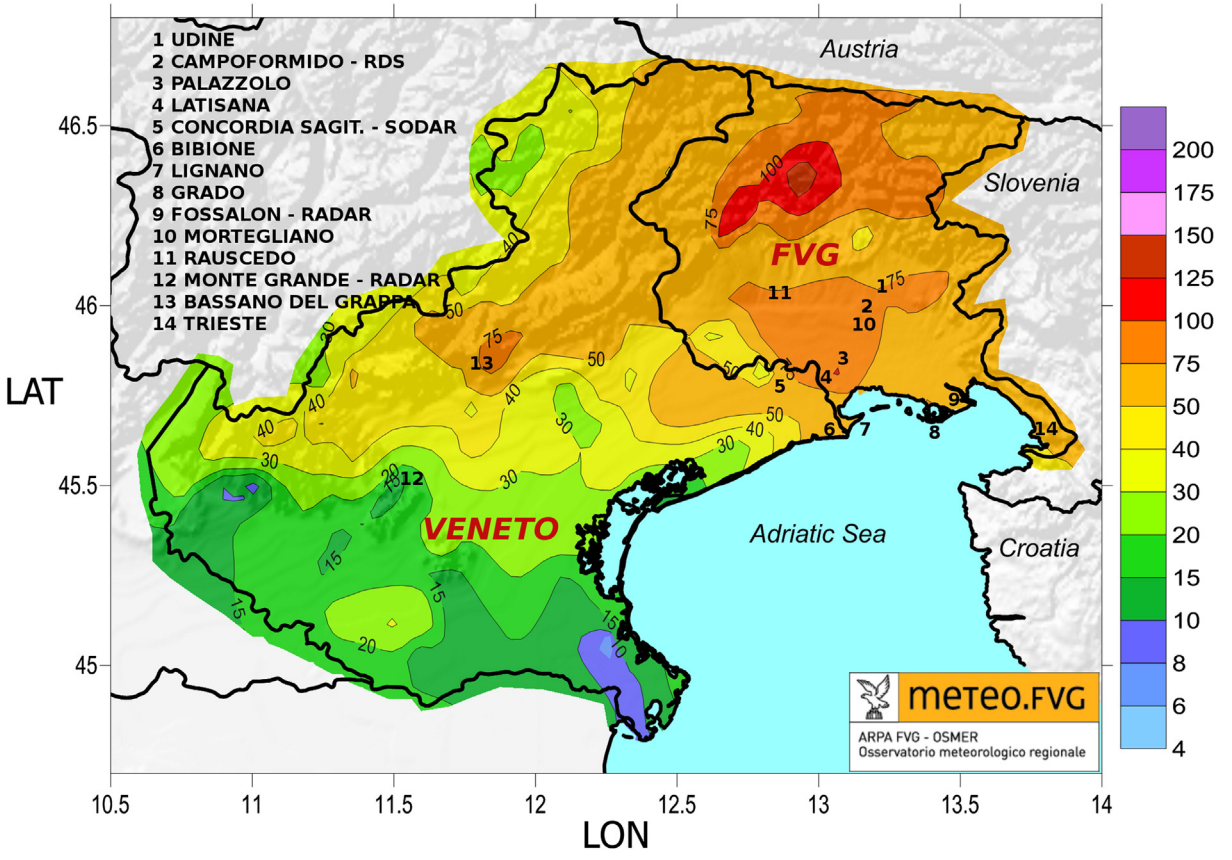

Fig. 1. Daily accumulated rainfall for 12 September 2012 in the Veneto and FVG regions, starting from 163 rain gauges in Veneto (ARPAV) and 111 rain gauges in FVG, spatialized with a natural neighbor method. All the locations quoted in the paper have been highlighted in the legend on the left side, including radar, sodar and radiosounding stations.
Courtesy of A. Cicogna (OSMER — ARPA FVG).

about 30 min in most of the stations managed by the Civil Protection.

Also the WMO 16044 radiosonde station is located in FVG (Campoformido, label "2" in Fig. 1) and managed by the Italian Air Force National Weather Service. This station launched 06 and 18 UTC "extra" soundings during the IOP2, in addition to the 1200 UTC and 0000 UTC standard soundings (Vaisala RS 92 radiosondes).

2.2. Remote sensing instruments

2.2.1. Ground-based remote sensing instruments (Doppler radars, sodar)

Among all the remote sensing instruments managed by CMT — ARPA Veneto, only the single polarization C-band Doppler radar located in Monte Grande – near Padova – and the Concordia Sagittaria Metek phased array sodar have been used in this work (see labels "12" and "5" in Fig. 1 for their location on the map).

A dual polarization C-band Doppler radar is also located in FVG (in Fossalon di Grado, label "9" in Fig. 1), managed by the regional Civil Protection, providing reflectivity, rain rate estimate and Doppler wind maps every 10 min.

2.2.2. Satellite image data

In addition to the standard Meteosat Second Generation (MSG) SEVIRI (Spinning Enhanced Visible and Infrared Imager) image data, taken at 15-min (regular full disc scan) and 5-min (Rapid Scan Service, RSS) intervals and covering the whole IOP2, for the early morning period (till 0900 UTC) additional experimental 2.5-min rapid scan data, taken with the MSG-3 satellite, were also available for the first time. This 2.5-min rapid scan experiment was conducted by EUMETSAT on 11 and 12 September 2012, during commissioning of the MSG-3 satellite (later renamed to Meteosat-10). For data availability and description of the experiment please refer to http://essl.org/cwg/?p=331.

2.3. Mesoscale models

During the SOP1, several modeling chains were run operationally by different institutions. Among the available high-resolution simulations, the forecasts of two mesoscale models, WRF and MOLOCH (described below), both implemented at CNR–ISAC, are employed here to complement the analysis.

2.3.1. WRF

The Advanced Research–Weather Research and Forecasting (WRF–ARW) model (see www.wrf-model.org; Skamarock et al., 2005) is a numerical system that solves the fully compressible, nonhydrostatic Euler equations. The model uses the terrain–following, hydrostatic–pressure vertical coordinate with vertical grid stretching. In the implementation used for HyMeX, the version 3.4 was used with forty vertical levels. Two daily runs were performed in real time, forced with Global Forecast System (GFS) analysis/forecasts, starting at 0000 and 1200 UTC. The outputs shown in this paper refer to the run initialized at 1200 UTC of 11 September 2012 in order to avoid any spin-up problem for the early hours of 12 September 2012.

Two domains were implemented: the largest domain, with a horizontal resolution of 15 km, covers approximately the northern part of the central Mediterranean basin (109 × 97 grid points), while the inner domain, one-way nested into the coarser grid, covers the northern Italy with a horizontal resolution of 3 km (206 × 206 grid points).

The WRF model contains different options for the parametrization schemes. In the model configuration used for HyMeX, the following schemes were selected: the Thompson et al. (2004) microphysics, which includes six classes of hydrometeor species plus number concentration for ice as prognostic variables; the Kain (2004) cumulus parametrization in the coarser grid (no parametrization is used in the inner grid); the Rapid Radiative Transfer Model (RRTM) for longwave radiation, based on Mlawer et al. (1997); the Dudhia (1989) scheme for shortwave radiation; the Monin–Obhukov–Janjic TKE scheme (Janjic, 2001) for the planetary boundary layer; and the Noah land–surface model (Niu et al., 2011).

2.3.2. MOLOCH

MOLOCH is a non-hydrostatic, fully compressible, convection resolving model developed at CNR–ISAC (Malguzzi et al., 2006). It uses hybrid terrain–following coordinate, relaxing smoothly to horizontal surfaces away from the Earth surface. Three dimensional advection is computed using the Eulerian Weighted Average Flux scheme (Billet and Toro, 1997).

The physical scheme consists of atmospheric radiation, subgrid turbulence, water cycle microphysics, and a soil model with vegetation. The atmospheric radiation is computed with a combined application of the Ritter and Geleyn (1992) scheme and the ECMWF scheme, employing 14 channels for the infrared and for the visible bands (Morcrette et al., 2008). The turbulence scheme is based on an E-l, order 1.5 closure, where the turbulent kinetic energy equation (including advection) is evaluated (Zampieri et al., 2005).

The microphysical scheme, recently upgraded, was initially based on the parameterization proposed by Drofa and Malguzzi (2004). The spectral properties of hydrometeors are simulated assuming a generalized gamma function distribution. The soil model uses seven layers and computes surface energy, momentum, water and snow balances, heat and water vertical transfer, vegetation effects at the surface and in the soil. It takes into account the observed geographical distribution of different soil types and soil physical parameters. For more details and references, refer to http://www.isac.cnr.it/dinamica.

In the operational implementation adopted during the SOP, the MOLOCH model was nested into a BOLAM (BOlogna Limited Area Model, also developed at CNR–ISAC) run initialized at 0000 UTC everyday, using GFS global model field as initial/boundary conditions. MOLOCH simulations (2.3 km horizontal resolution) started at 0300 UTC and run for 45 h over a domain including the entire Italian territory and surrounding seas (about 530 × 578 grid points and 50 vertical levels).

3. Description of the 12/09/2012 events

During 12 September 2012, three series of storms – separated by a few hours each other – hit NEI and in particular the eastern part of Veneto region and the plain of FVG region. During the morning, the first systems produced a supercell signature and a strong hailstorm near Latisana (see label "4" in Fig. 1). Five hours later, another large storm produced a funnel cloud near Mortegliano (label "10" in Fig. 1). Lastly, between 1700 and 1800

UTC a third "elongated" storm moved along the North Adriatic coast. Here follows a detailed description of the three events.

3.1. Synoptic and mesoscale description

The anomalously warm conditions that affected the late summer of 2012 produced high temperatures also during the first days of September. Therefore, FVG region was characterized by positive anomaly in both sea surface temperature (SST) and low level troposphere temperatures (OSMER internal report "meteo.fvg September 2012" http://www.meteo.fvg.it/pubblicazioni.php). From a synoptic point of view, these conditions were ascribable to a persisting anticyclonic ridge, that extended poleward from the Mediterranean basin to the Scandinavian Peninsula. Such a blocking phase was interrupted in the evening of 11 September, when a North Atlantic trough intruded into the western part of the ridge, inducing the advection of cooler air toward northern Italy.

At 0600 UTC of 12 September a shallow orographic cyclone developed on the lee side of the Alps, with two surface centers, one over the Genoa Gulf and the other one over the eastern Po Valley (Fig. 2). The latter low pressure system was displaced eastward by the ascending branch of the trough aloft, preceded by a moderate southerly flow in the lowest troposphere. The low level winds blowing from the Adriatic Sea toward the eastern Alpine ridge advected warm and moist air over FVG region, where potential instability progressively increased. The unstable flow of warm and moist air at low layers appeared determinant also in other heavy rain events in the Mediterranean area (e.g. Riesco Martin et al., 2013). At 1200 UTC the synoptic trough moved southeastward driving a potential vorticity advection and a divergent flow at 300 hPa over the eastern Po Valley. Then, in the late afternoon, the sharp pressure gradient across the Alpine ridge resulted in strong and cooler northerly winds descending along the Alpine slopes and spreading into Veneto and FVG plains immediately after the cold front passage at 1800 UTC.

Fig. 3a shows the time-series of the Campoformido soundings in the lowest 7 km a.m.s.l. with some instability indices (Convective Available Potential Energy – CAPE –, Convective INhibition – CIN – and Level of Free Convection, LFC) computed from the high-vertical-resolution soundings by the Sound_Analys.PY software (Manzato and Morgan, 2003). Considerable potential instability was present, particularly between 0000 and 0600 UTC of 12 September. The sounding at 0600 UTC shows high potential instability with respect to the climatological values (mid-September is toward the end of the thunderstorm and hail season in FVG), although the Lifted Index (calculated using the mean air of the first 500 m, as defined by Galway, 1956) is only −0.7 °C. Anyway, the difference of temperature between environmental temperature at 500 hPa and the Most Unstable Parcel (θ_e = 336 K located at 800 m a.m.s.l.) lifted pseudo-adiabatically at 500 hPa was as high as DT500 = −5.0 °C, while CAPE was almost 1680 J/kg (or 1880 J/kg using the virtual correction) and precipitable water was 34 mm.

At 0600 and 1200 UTC, southeasterly wind affected the lowest 1.5 km, while the wind blew from W or SW aloft. On the

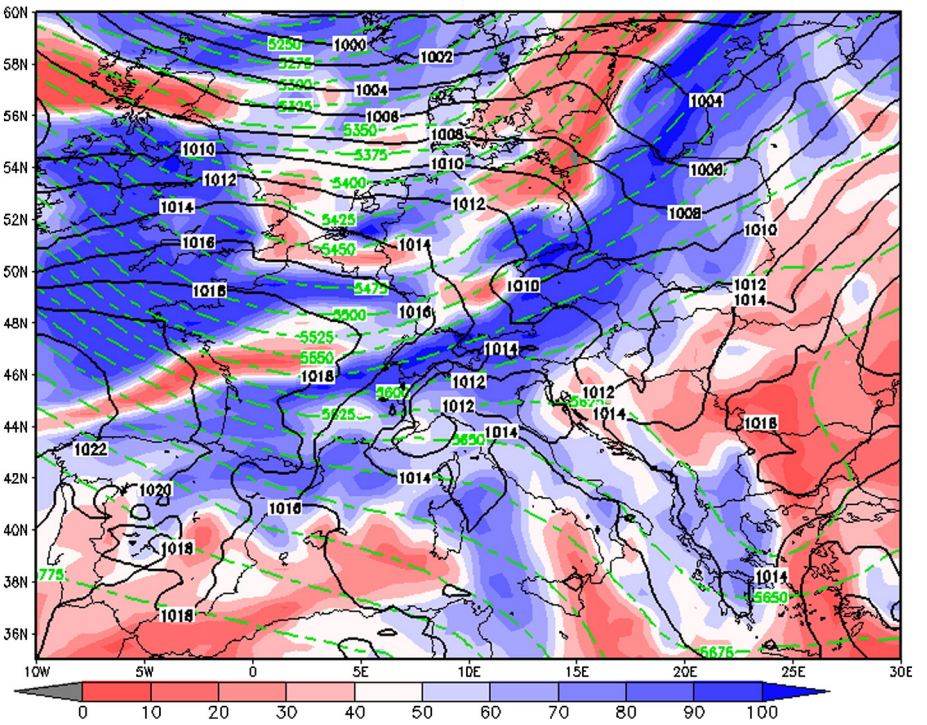

Fig. 2. Synoptic situation at 0600 UTC, 12 September 2012. 500 hPa geopotential height (green dashed lines), 700 hPa relative humidity (shaded field in red/blue) and mean sea level pressure (black solid lines).
Source: ECMWF deterministic run of 12 September 2012 at 00 UTC, +6 h forecast.

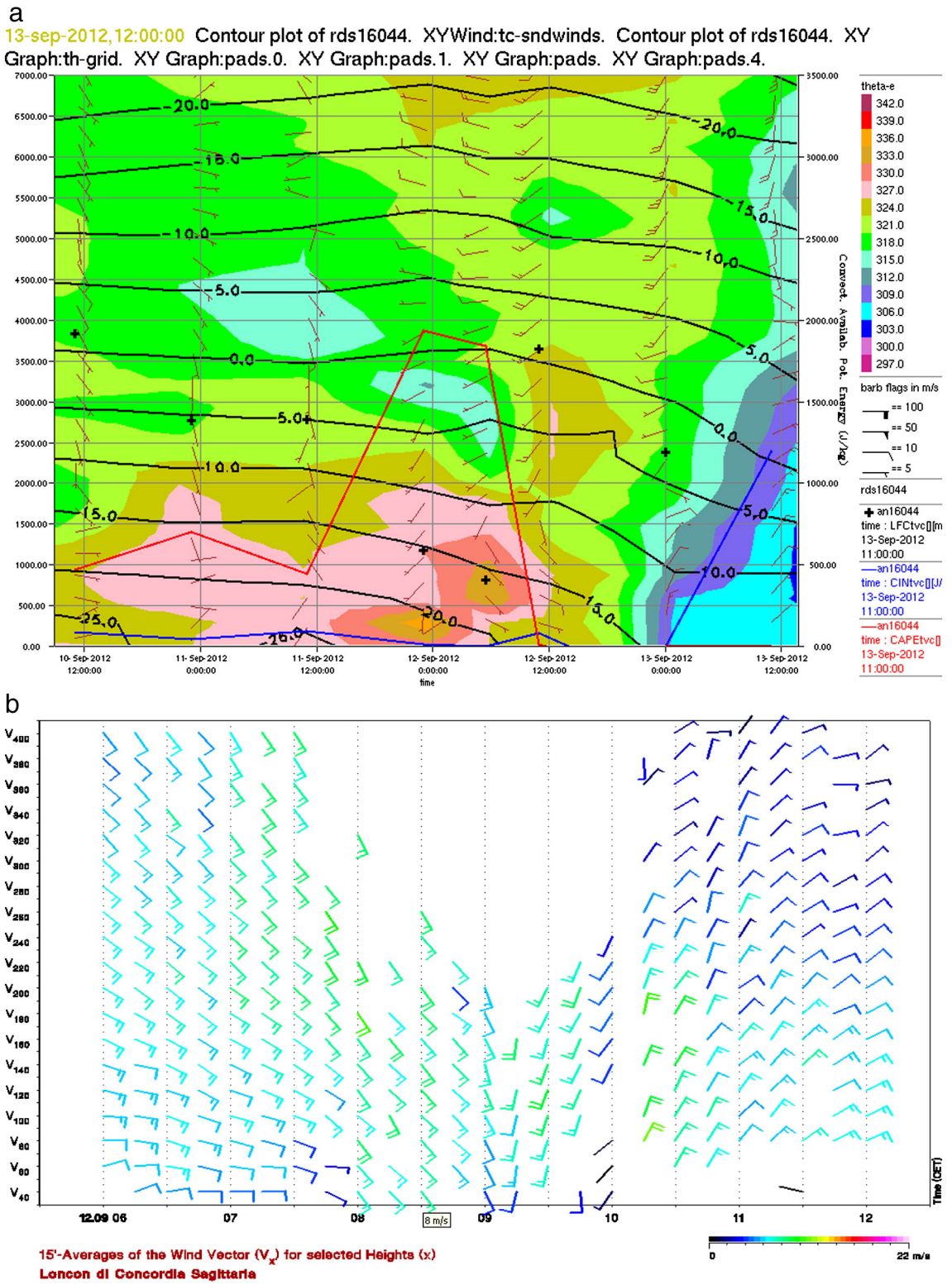

Fig. 3. a. Vertical-time series in the lower 7 km (left scale in [m]) of all the Udine soundings launched by Aeronautica Militare between 1200 UTC of 10 September and 1200 UTC of 13 September, with horizontal winds and Θ_e in shaded colors (colorbar scale). Superimposed are CAPE and CIN estimations (right scale in [J/kg]) as lines, while LFC (Level of Free Convection) as "+" (displayed by the NCAR "Zebra" software). b. High resolution data of Concordia Sagittaria SODAR in the lowest 400 m between 0500 and 1100 UTC; note that the hour in the axis is expressed as UTC + 1 h. (For interpretation of the references to color in this figure legend, the reader is referred to the web version of this article.)

contrary, at 0000 UTC of the following day – after the passage of the front – the low level wind blew from N or NE, while still remained from SSW above. Also the abrupt change of Θ_e during the afternoon of 12 September is a clear sign of the cold front passage.

Fig. 3b shows the wind time-series recorded by the Concordia Sagittaria (Loncon, label "5" in Fig. 1) sodar from 0500 to 1100 UTC of 12 September 2012. The observed horizontal wind profile shows a period (0700–0900 UTC) characterized by a low level moist southerly jet from the Adriatic Sea. The maximum intensity of this southerly wind is about 8 m/s at 0730 UTC. Note also the abrupt change in wind direction after 0900 UTC. A similar effect can be identified looking at the daily evolution of 10 m wind observed at the coastal station of Bibione (label "6" near the coast in Fig. 1, not shown).

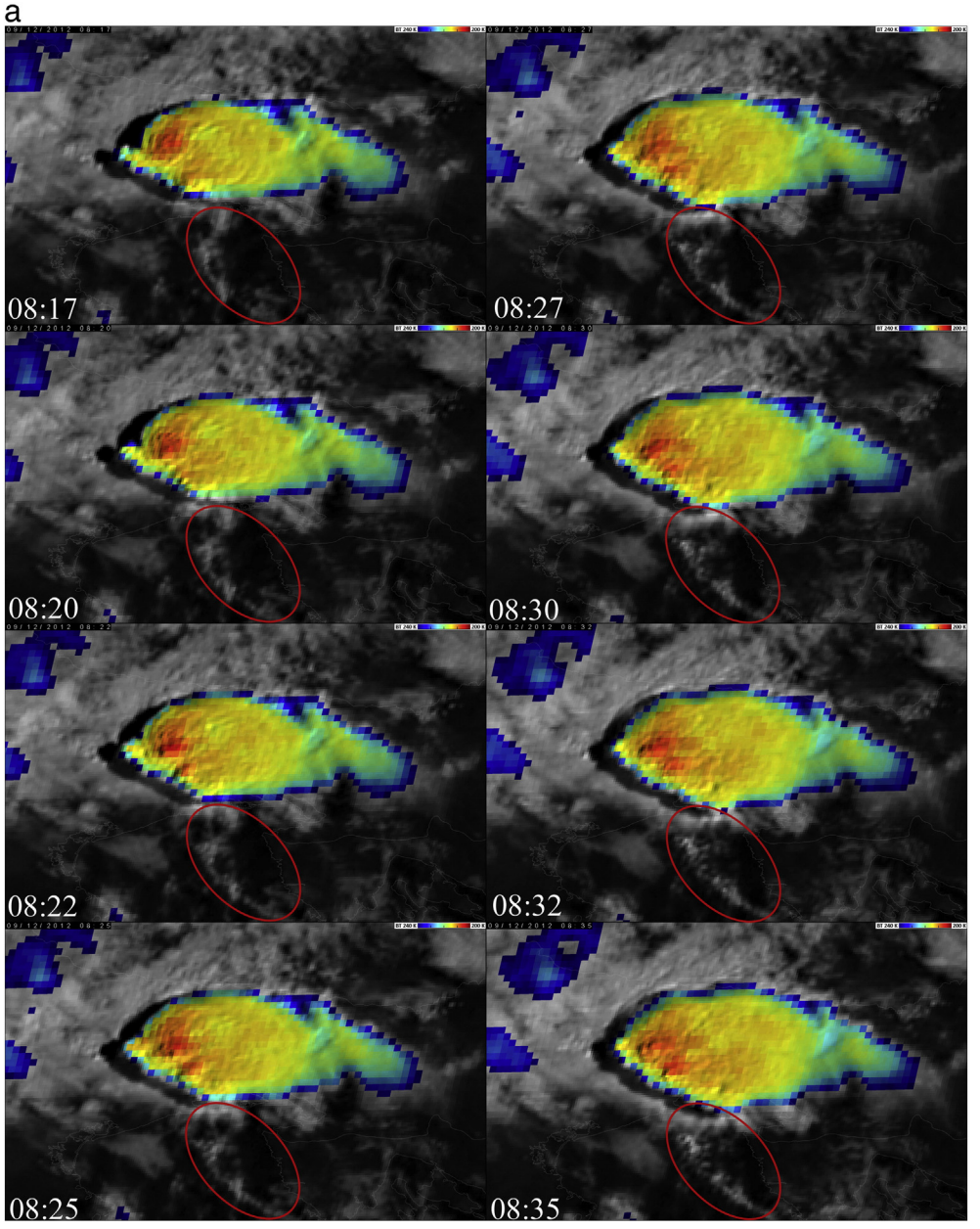

Fig. 4. a. Sequence of satellite images ("sandwich" product, based on HRV and IR10.8-BT 200–240 K bands) documenting the evolution of the storms between 0817 and 0835 UTC of 12 September 2012, captured by MSG-3 (Meteosat-10) satellite in experimental 2.5-minute rapid scan mode. The red ellipse shows the area of low level convergence, feeding the inland convection. Details of the evolution are discussed in the text. Note that these images are not parallax-corrected. Data provided by EUMETSAT. b. As Fig. 6a but from 0837 to 0855 UTC of 12 September 2012. (For interpretation of the references to color in this figure legend, the reader is referred to the web version of this article.)

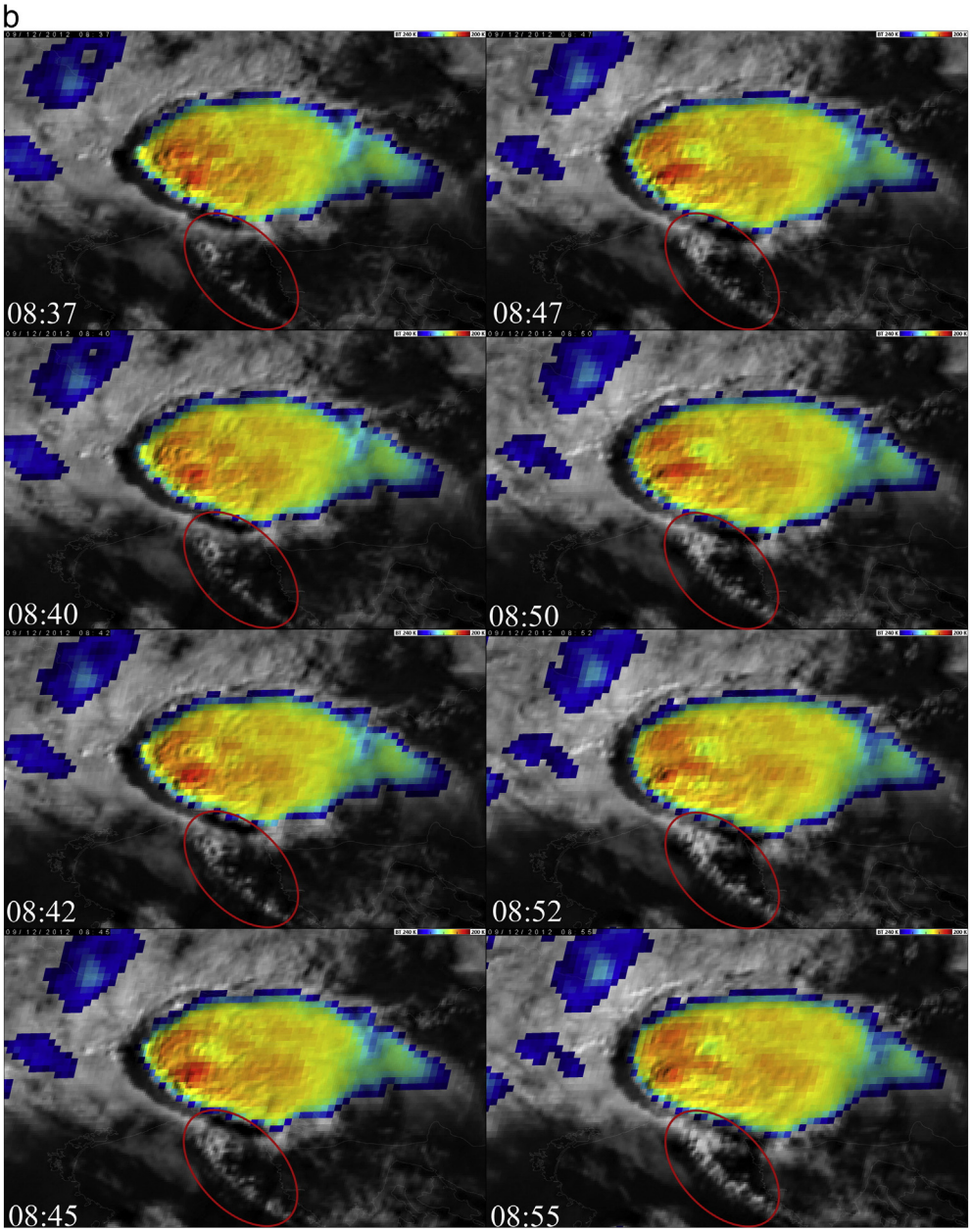

Fig. 4 (*continued*).

3.2. 0800–1100 UTC: "Rauscedo–Latisana–Grado" supercell

Fig. 1 shows also the spatialized – with a natural neighbor algorithm – distribution of accumulated daily rainfall, as observed by all the surface stations. The maximum value in Veneto region was recorded near Bassano del Grappa (label "13" in Fig. 1) with 97 mm in 24 h (of which 53 mm in only 1 h, between 1300 and 1400 UTC). On the other side, there are some other higher maxima in the FVG region: the highest peak is in the Carnic Alps (up to 158 mm in 24 h), while a secondary maximum is in the plain (values up to 103 mm in 24 h observed at 10 km on the west side of Campoformido, label "2"). The hourly rain rate of 52 mm measured between 0900 and 1000 UTC in the Palazzolo station (label "3") is also notable.

The precipitation peak in the FVG plain is – at least for the main part – associated with two different thunderstorms developed in the morning, which will be called hereafter as the "Northern storm" (affecting more the Rauscedo area, label "11") and the "Southern storm" (affecting more the area near Latisana, label "4"). The Northern storm was already developed at 0630 UTC (0830 local time) affecting the area near Rauscedo, in the western part of FVG, while it started to move to SE (toward Latisana) after 0800 UTC. In contrast, the Southern storm started at about 0750 UTC near Concordia Sagittaria

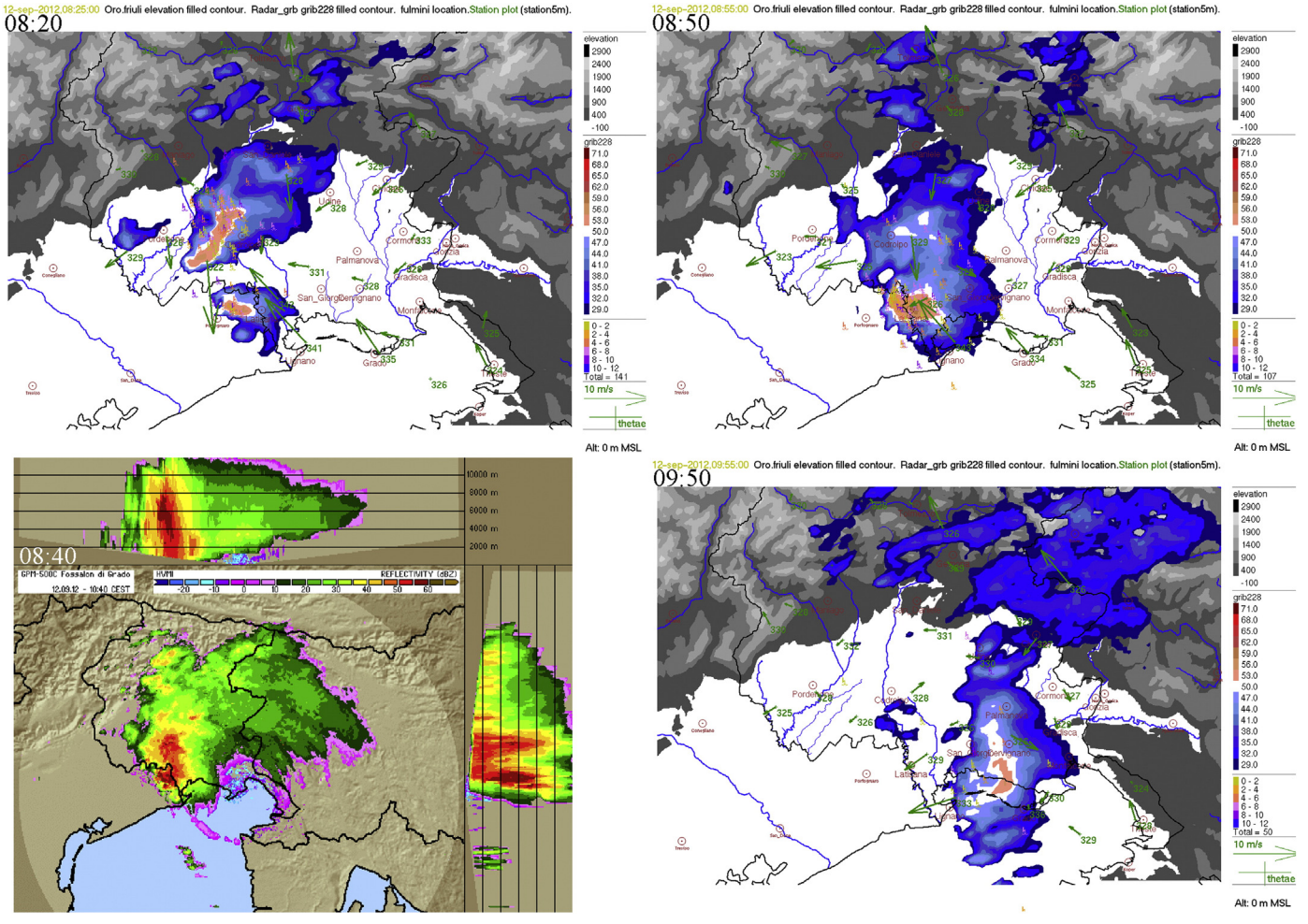

Fig. 5. Vertical Maximum Intensity (VMI) of the reflectivity measured by the Fossalon di Grado radar, with Θ_e (red–blue colorbar in dBZ) and 10-m wind observed by surface stations (5 min time resolution) and the CESI-Sirf cloud-to-ground lightnings within the ± 6 min interval (colorbar shows time delay in minutes) at 0820, 0850 and 0950 UTC (a, c and d respectively). (b) Fossalon radar maximum reflectivity at 0840 UTC vertical (VMI) and lateral projections (HVMI). (For interpretation of the references to color in this figure legend, the reader is referred to the web version of this article.)

(label "5", in the northern Adriatic coastal area of Veneto) and moved to NE (also toward Latisana).

The evolution of these early morning storms was well captured by the MSG-3 satellite with its experimental 2.5-minute "super" rapid scan mode. Fig. 4a and b show respectively the images from 0817 UTC to 0835 UTC, and from 0837 UTC to 0855 UTC (when the 2.5-minute rapid scan was completed), with one frame every 2.5 min. This corresponds to the most interesting part in the evolution of the systems, when the Northern storm weakened and the Southern one gained on its maximum intensity. The sequence shown in Fig. 4 consists of series of "sandwich" images (Setvák et al., 2012), which are based on HRV and color-enhanced IR10.8 bands, with its brightness temperature (BT) ranging from 240 K (in blue) to 200 K (red).

As shown in Fig. 4, at the beginning of this series (0817 UTC) the Northern storm dominated (larger area of significantly lower BT, more overshooting top, hereafter OT, activity), while a weaker and smaller cell can be seen southeast of the dominant one. At 0822 UTC the Southern storm generated the first significant, cold OT, which however weakened shortly after. Then, the Southern storm generated a new, more distinct OT at about 0835 UTC, when also the Northern storm was still quite active. However, later on, the satellite images clearly indicate that the Northern storm quickly weakened (no more OTs after 0837 UTC), while the Southern storm became the dominant one, generating cold OTs till the end of the sequence, at 0855 UTC. In addition to the overshooting tops, the images also show an embedded warm area, which formed downwind (NE) of the Southern storm and remained persistent till the end of the period, and also a cold above-anvil plume, that can be seen first at 0847 UTC.

The following evolution of the storms, beyond 0900 UTC, was documented by the regular 5-minute rapid scan service (RSS, not shown here). The storms remained active (from the satellite perspective) till about 1100 UTC, dissipating quickly afterward. Besides the storm evolution itself, the series of Fig. 4 panels documents also the usefulness of the 2.5-minute super RSS, as some of the features described above can only be traced for a very short period.[2]

Kerkmann et al. (2012) provided additional satellite images and namely the image loops documenting the full evolution of these storms. They also proposed the hypothesis that the Northern storm was generated by a southeasterly moist low level wind (Scirocco), blowing from the northern Adriatic Sea toward the orographic barrier of the Carnic Prealps. In Fig. 4 the red ellipse highlights the area where the moist convergence line – feeding the inland storms – was confined. Analyzing the super RSS satellite images before 0817 UTC (not shown) it is possible to identify a thin convergence line in that area starting already at 0730 UTC,[3] just before the Northern storm started to move toward south. So, the convergence line remained almost stationary above the northern Adriatic Sea from 0730 to 0910 UTC (see also the change in wind direction after 0900 UTC in Fig. 3b) and then it moved faster eastward (almost in parallel with the Southern storm) and was also able to trigger new cells after 1000 UTC inside the Istrian peninsula.

This mesoscale situation is well depicted and confirmed by the radar reflectivity data shown in Fig. 5. Fig. 5a shows the 0820 UTC Vertical Maximum Intensity (VMI, the maximum radar reflectivity on each vertical column projected on a horizontal map) of the Fossalon di Grado radar and the surface station measures at 0825 UTC, overlapped with the cloud-to-ground lightning in the previous 12 min (source CESI–SIRF). The equivalent potential temperature (Θ_e) registered in the coastal station of Lignano (label "7" in Fig. 1) was 341 K, while it reached 342 K in Palazzolo (label "3"). These values were much higher than those registered in the surrounding area, thus confirming the presence of a localized low level southerly high-Θ_e flux (warm tongue) feeding the storms. Also their 10-m winds, blowing from the SE, are stronger than those observed in the other stations.

Fig. 6 shows the evolution between 0800 and 0945 UTC of the Fossalon (label "9" in Fig. 1) Doppler radar field, as seen by the Lowest Beam Map (LBM, incoming velocities in red and outcoming velocities in blue). Already at 0800 UTC the Northern cell exhibits a mesocyclone signature (inside the yellow circle). An abrupt change in the Northern storm trajectory happened at about this time, when the cell started to deviate by about 75° to the right with respect to the environmental mean wind (see more details in Section 5). The mesocyclone signature associated with the Northern storm seems to persist until 0845 UTC. After that (0900, 0915 and 0945 UTC) it is more difficult to say if the ingoing–outgoing velocity couplets were related to a rotating structure or – more probably – to a linear advection of the – eastward – storm downdraft that protruded inside the – westward – environmental wind.

The Southern storm intercepted the trajectory of the Northern one at about 0830 UTC, cutting the southerly feeding flow, as suggested also by Kerkmann et al. (2012). This evolution produced a sudden reinforcement of the Southern storm, at the expense of the Northern one, as shown at 0840 UTC in Fig. 5b (HVMI, that is VMI map plus the horizontal maximum reflectivity projected on two lateral sides). It is worth noting a core of maximum reflectivity of about 55–60 dBZ located between 4000 and 6000 m a.m.s.l. Even if at that time the Southern storm seems to exhibit rapidly developing long-lived overshooting tops (resulting from vigorous updrafts) as discussed above and the maximum reflectivity of the Northern cell was decreasing, the Doppler LBM at 0845 UTC of Fig. 6c identifies a mesocyclone signature that was still well co-located with the VMI associated to the Northern cell. For all these reasons the Northern storm after 0800 UTC could be classified as a supercell.

Vertical sections derived from the Fossalon di Grado and from the Monte Grande (label "12" in Fig. 1) radar PPI images indicate that the maximum reflectivity values (above 60 dBZ) were located at about 5 km a.m.s.l. (not shown), while the cloud base was very low – about 500 m a.m.s.l. – and the cloud top was estimated above 13 km. The tropopause height derived by Campoformido 0600 and 1200 UTC soundings was estimated to be between 11.2 and 11.6 km a.m.s.l., so the cloud top was overshooting well above the tropopause.

[2] The 2.5-minute super rapid scanning will be operationally implemented at the Meteosat Third Generation satellites See http://www.eumetsat.int/website/home/Satellites/FutureSatellites/MeteosatThirdGeneration/index.html.

[3] It should be noted here that the first weak signal of this convergence line above the Adriatic Sea is visible in Doppler radar field only 40 min later (not shown).

At 0850 UTC VMI was already below 50 dBZ in the Northern cell, as visible in Fig. 5c (compare also with the last two satellite frames of Fig. 4b), but just before 0900 UTC the presence of a lot of medium-sized hail was reported on the A14 highway near Latisana. The Doppler radar image at 0900 UTC (Fig. 6d) shows a couple of positive and negative radial velocities just on the eastern side of Latisana, but it is not possible to discriminate if it is a signature of rotation or just a convergence between horizontal winds with opposite directions, because the sharp boundary between these red and blue areas is orthogonal to the Fossalon radar radius.

The convergence line elongated over the northern Adriatic Sea, as seen by the Doppler LBMs velocities of Fig. 6, became stronger from 0900 to 0945 UTC. This increase of the "red tongue" velocity shown by the Doppler sequence could also be due to an apparent effect, i.e. the orientation of the line with respect to the radar radius (the radar location in Fossalon, label "9", is quite close). In any case, this line of strong incoming velocities (larger than 10 m/s after 0915 UTC) tracked the moist unstable inflow feeding the inland convective systems and moved together with it. In fact, looking carefully at all the available VMI and Doppler frames, it seems that both the Southern cell and the convergence lines were pushed eastward by a meso-scale cold front, that could be associated to the meso-low simulated above Venice by the LAM forecast (as will be described in Section 4).

Interestingly, after the Southern cell became wider and the Northern cell weakened, the Southern cell evolved from its original circular-shaped structure shown in Fig. 5c. An arc-shaped echo in the VMI field was evident at 0950 UTC (Fig. 5d), suggesting its evolution into a small bow-echo-like structure (Atkins and St. Laurent, 2009), sustained by strong winds (note the corresponding strong incoming Doppler wind – generating folding – of Fig. 6f). From this point of view, the LBM Doppler radar wind maps of the inland cell (Fig. 6d–f) suggest that a cold rear inflow jet behind the red line (tracking the meso-scale front air) moved beneath and inside the warmer air near the surface. The forecasters of FVG regional meteorological service reported similar evolutions over the Grado lagoon in past episodes (e.g. Pucillo and Manzato, 2010 on the 08/08/08 bow-echo-like Grado storm). These considerations suggest a possible mechanism for enhancing deep convection in this particular area, that is, the possibility that warmer air near the lagoon and moist flux coming from the northern Adriatic Sea might have emphasized the temperature contrast of a small cold front moving eastward.

3.3. 1400–1530 UTC: "Portogruaro–Mortegliano" supercell

Convective activity in the NEI area reactivated during the afternoon. Thunderstorms occurred at about 1300 UTC near the city of Treviso, while at 1400 UTC an extensive storm was present in the vicinity of Portogruaro (near Venice). Fig. 7a clearly shows the maximum VMI above 60 dBZ at 1400 UTC, associated with this storm, which lasted for about two hours, while moving toward E-NE.

Also, a small signature of rotating structure is displayed by the Doppler LBM field at about 1420 UTC near Portogruaro (Fig. 7b). Then, the storm reached Mortegliano at about 1530 UTC where a storm chaser took the picture of a rotating wall cloud and funnel-cloud (not shown, but available at Marko Korosec's web site http://www.weather-photos.net/gallery/thumbnails.php?album=416). As the funnel did not reach the ground, it cannot be classified as a tornado from this picture. Although at that time the Doppler LBM did not show any mesocyclone signature, the observations above indicate that also this storm probably was a supercell.

3.4. 1700–1830 UTC: "Portogruaro–Grado" squall-line

Later in the evening, at about 1700 UTC, a convective cell producing a high reflectivity signature (above 52 dBZ) formed south of Portogruaro and moved along the coast toward E-NE. In front of this storm, the coastal area was affected by SE flow characterized by high Θ_e values, up to 337–338 K in Lignano and Grado (labels "7" and "8" in Fig. 1) respectively, as shown in Fig. 8a. One hour later the main storm was above the sea, but displaying an elongated shape directed inland (Fig. 8b). This was associated with a sudden drop of about 10 K in the values of Θ_e observed by many surface stations (not shown) over the plain. Another Θ_e drop, although less steep, of about 15 K was recorded a few hours later (steady decrease of Θ_e from 2100 to 0000 UTC of 13 September, not shown).

The corresponding Doppler LBM of the Fossalon di Grado radar (not shown) does not show any evident mesocyclone signature, but confirms only the presence of strong winds that probably caused folding problems. That corresponds to an increase of the radial wind speed blowing from SW above 12 m/s. Therefore, this storm can be classified as severe weather event for sure, although likely not a supercell.

4. LAM simulations

The ability of the models to reproduce the complex meteorological evolution characterizing the HyMeX IOP2, thus supporting the meteorological analysis, is discussed in this section.

Both models (MOLOCH and WRF) reproduce properly the convective activity triggered over the Alpine foothills in the first phase of the IOP, although they missed the exact temporal evolution and location of the cells. The upstream sounding simulated with the WRF model at 0000 UTC of 12 September (initialized at 1200 UTC of the day before) at the gridpoint 46.00°N, 13.00°E (Fig. 9a) shows a southeasterly wind component, confined to the lower 1000 m, consistent with the observations, and a weak inhibition (CIN = 20 J/kg). The atmosphere was potentially unstable. In fact, the most unstable parcel, located a few hundred meters above the surface, had a CAPE of approximately 800 J/kg. Six hours later (Fig. 9b), the value of some instability indices simulated with WRF in the same location became worth of attention: the inhibition was no longer present, CAPE increased to about 1300 J/kg (the "Most Unstable Lifted Index" was −5 °C), the Total Totals was equal to 50, a value generally associated to scattered severe thunderstorms and isolated tornadoes.

Both models are able to reproduce some mesoscale features that possibly played an important role in feeding the convective systems during this phase, i.e. a tongue of warm air advected by an intense SSE moist and warm low level jet (LLJ), confined to the eastern flank of the Adriatic Sea. One can identify the convergence among three different flows (Fig. 10): 1. the SSE moist LLJ from the Adriatic Sea; 2. the ENE barrier

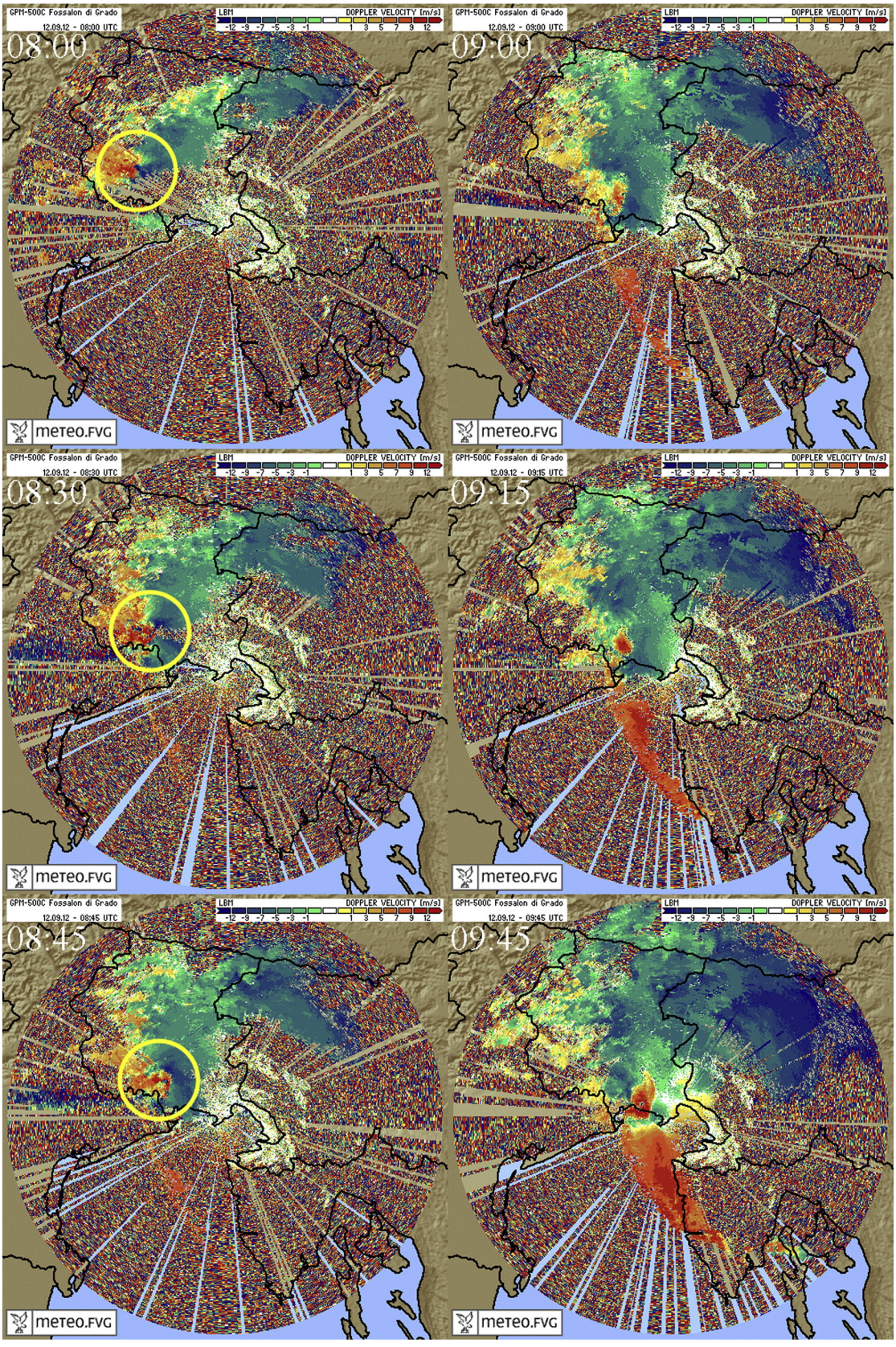
GPM-500C Fossalon di Grado
12.09.12 - 08:00 UTC
08:00
LBM
DOPPLER VELOCITY [m/s]
-12 -9 -7 -5 -3 -1 1 3 5 7 9 12
meteo.FVG
GPM-500C Fossalon di Grado
12.09.12 - 09:00 UTC
09:00
LBM
DOPPLER VELOCITY [m/s]
-12 -9 -7 -5 -3 -1 1 3 5 7 9 12
meteo.FVG
GPM-500C Fossalon di Grado
12.09.12 - 08:30 UTC
08:30
LBM
DOPPLER VELOCITY [m/s]
-12 -9 -7 -5 -3 -1 1 3 5 7 9 12
meteo.FVG
GPM-500C Fossalon di Grado
12.09.12 - 09:15 UTC
09:15
LBM
DOPPLER VELOCITY [m/s]
-12 -9 -7 -5 -3 -1 1 3 5 7 9 12
meteo.FVG
GPM-500C Fossalon di Grado
12.09.12 - 08:45 UTC
08:45
LBM
DOPPLER VELOCITY [m/s]
-12 -9 -7 -5 -3 -1 1 3 5 7 9 12
meteo.FVG
GPM-500C Fossalon di Grado
12.09.12 - 09:45 UTC
09:45
LBM
DOPPLER VELOCITY [m/s]
-12 -9 -7 -5 -3 -1 1 3 5 7 9 12
meteo.FVG

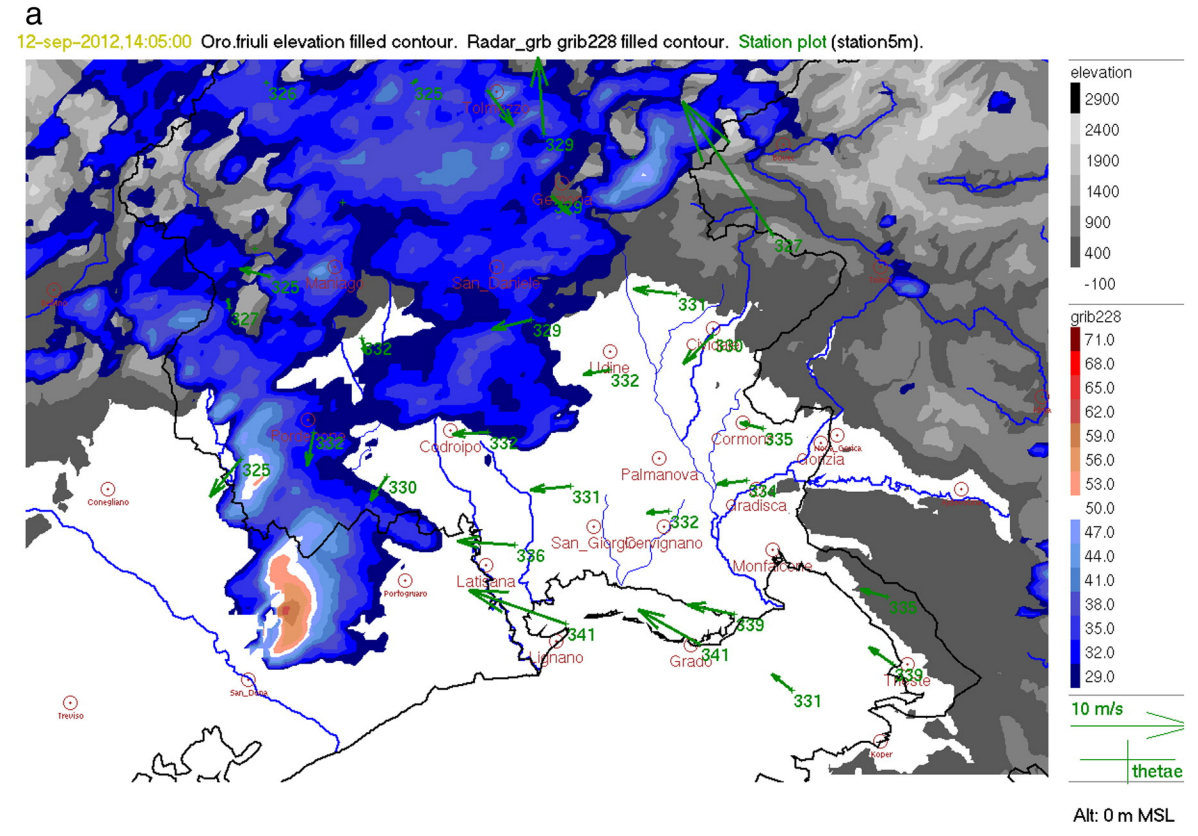

Fig. 7. a. VMI in dBZ (red–blue colorbar) at 1400 UTC as measured by the Fossalon radar with 5′ surface data at 1404 UTC and cloud-to-ground lightnings (source CESI–SIRF). b. LBM Doppler at 1420 UTC of the Fossalon radar. The yellow circle encloses a possible small wind signature of rotation. (For interpretation of the references to color in this figure legend, the reader is referred to the web version of this article.)

flow ahead of the Alpine chain – just inland –, generated by the orographic deflection of the SSE wind from the sea; 3. the SW wind over the Italian northern Adriatic coast, which turned to westerly over the Adriatic Sea. As displayed in the Bologna radiosounding (WMO 16144, not shown) at 1200 UTC, the latter flow was Apennines foehn, characterized by dry adiabatic lapse rate and low values of relative humidity in the lower layers.

Such convergence was able to trigger ascending motion well upstream of the foothills and can be considered as responsible for convective initiation. Also, the gradient in Θ_e can be similarly ascribed to the coexistence of the SSW drier flow from the Apennines with the LLJ. A filament of high θ_e around 340 K reached the inland region and compares well with the observed values (see Section 3.2). As a consequence, high values of CAPE (larger than 2000 J/kg, not shown) were present along the foothills, producing conditions extremely favorable to orographic triggering of convection.

This mesoscale circulation was probably driven by a shallow low pressure system centered over the Venice Lagoon in the morning and clearly displayed in the MOLOCH forecast (Fig. 10). The presence of a pressure gradient in the lowest levels, although quite weak, probably played a role in confining and intensifying the LLJ on the eastern side of the Adriatic (that is, the convergence line highlighted also in Fig. 4).

Although reproducing pretty well the mesoscale environment, both models miss the exact development of the two convective systems. In particular, MOLOCH correctly predicts the Southern storm both in terms of timing and location, but misses the Northern one (Fig. 11a). On the opposite, WRF captures both cells in the simulated reflectivity field, but predicts, incorrectly, that the Northern cell is more intense than the Southern one. Also, their movement was more zonal than observed, and the evolution was simulated with a delay of few hours (Fig. 11b). The different evolution of the storms simulated by the two models can be ascribed to the different penetrations of the LLJ: at the time of the triggering of the Northern storm, the WRF model predicts an intensification of the jet and its extension farther northward, up to the foothills, while in MOLOCH the inflow remained more confined close to the coastline, where it produced an intense convergence

Fig. 6. LBM Doppler at 0800, 0830, 0845, 0900, 0915 and 0945 UTC of 12 September 2012 (a, b, c, d, e and f respectively) of the Fossalon radar. The yellow circle encloses a wind signature resembling a rotating structure (mesocyclone). At 0830, 0845 and 0945 UTC there is a folding spot inside the red maxima. (For interpretation of the references to color in this figure legend, the reader is referred to the web version of this article.)

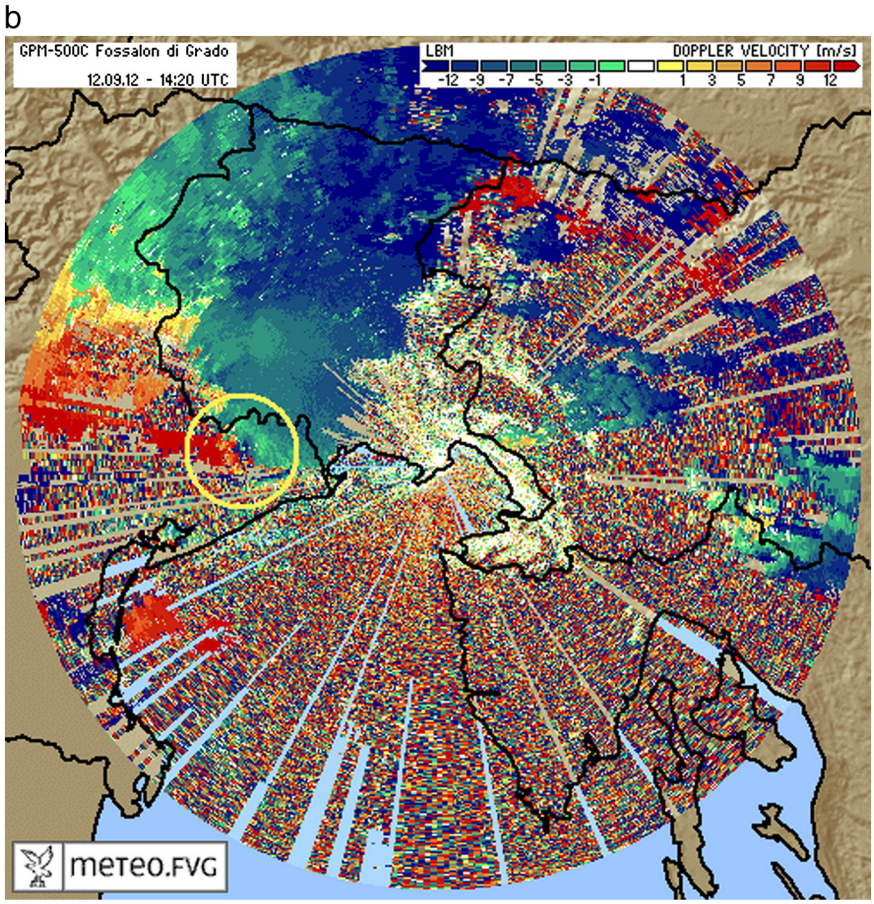

Fig. 7 (*continued*).

associated with the highest Θ_e values. This difference was partly due to the shallow cyclone over the Venice Lagoon, whose associated circulation (Fig. 10) was more intense in MOLOCH than in WRF forecast and affected the wind coming from the Adriatic Sea, producing a stronger cyclonic curvature in correspondence to the FVG coastal area.

WRF model reproduces some graupel (not shown) extending up to tropopause in the plain area near Udine (label "1" in Fig. 1), associated with the occurrence of hail near Latisana, although shifted northeastward. The convective line emerging in the radar reflectivity images over the Adriatic Sea later in the morning is not simulated by any model, although MOLOCH shows a clear signature of saturated air in the lower troposphere, feeding the convection, and the WRF model simulates a small tongue in the 850 hPa relative humidity protruding into the Adriatic Sea (not shown).

The second phase is not well reproduced by any model. Some weak rainfall was generated more to the west, in Veneto region, in the WRF model simulations, while MOLOCH forecasts some intense thunderstorms in correspondence with the Alpine foothills. However, both the location and intensity are not correct. The triggering mechanisms of these scattered convective cells over the eastern Po Valley seem to be associated with local thermal factors, in the absence of any intense synoptic or organized mesoscale forcing. For this reason the development of this convective activity is possibly characterized by a low predictability.

During the third phase of the event, in the afternoon, the SSE flow along the coast rapidly changed, becoming NW in the evening, due to the arrival of cold air crossing the Alps. Compared with Concordia Sagittaria sodar measurements, both models reproduce this rapid transition even if MOLOCH shows a better agreement with the observations. An intense cell developed to the south of Portogruaro (Fig. 8a), moving along the coast toward E-NE; one hour later a convective system resembling a squall line crossed the Adriatic Sea and the coastal region (Fig. 8b). The line over the sea can be clearly identified in the rainfall field, relative humidity and cloud water/ice content of the MOLOCH simulation (Fig. 12a). Ahead of the storm, a SE flow associated with high Θ_e values (up to 338 K) still affected the coast, but a sharp cold air katabatic flow progressively penetrated into the Po valley and then into the northern Adriatic (Fig. 12b).

The mesoscale forcing, due to cold northerly winds descending from the Alps, was intense and affected quite a wide area: therefore, both models are able to reproduce the intense convective activity, although the speed and the location of the convective line is different for the two simulations. Comparing the forecast fields (Fig. 12a and b) it is possible to

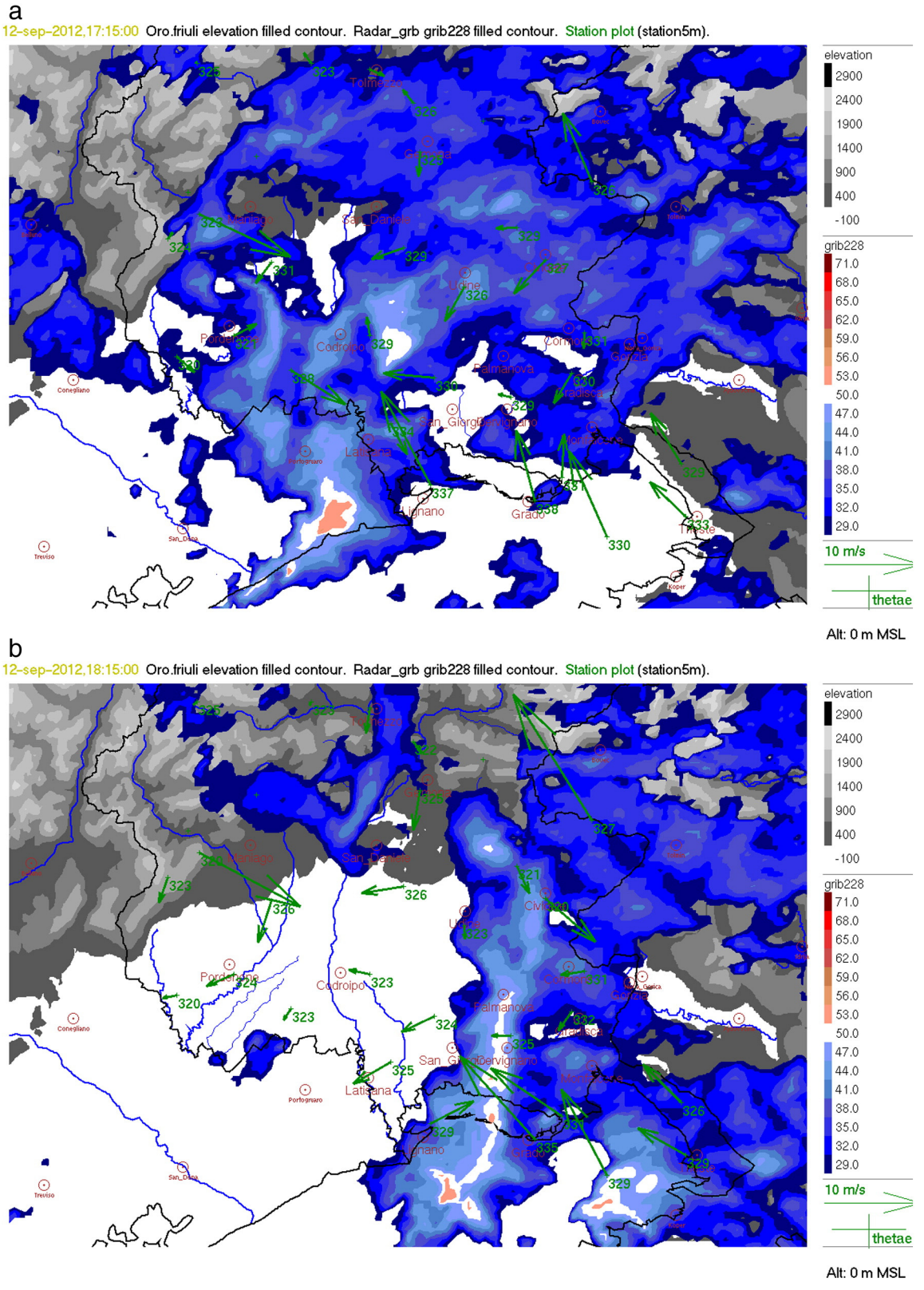

Fig. 8. a. VMI at 1710 UTC as seen by the Fossalon radar with 5′ surface data at 1715 UTC and cloud-to-ground lightnings (source CESI–SIRF). b. VMI at 1810 UTC as seen by the Fossalon radar with 5′ surface data at 1815 UTC and cloud-to-ground lightnings (source CESI–SIRF).

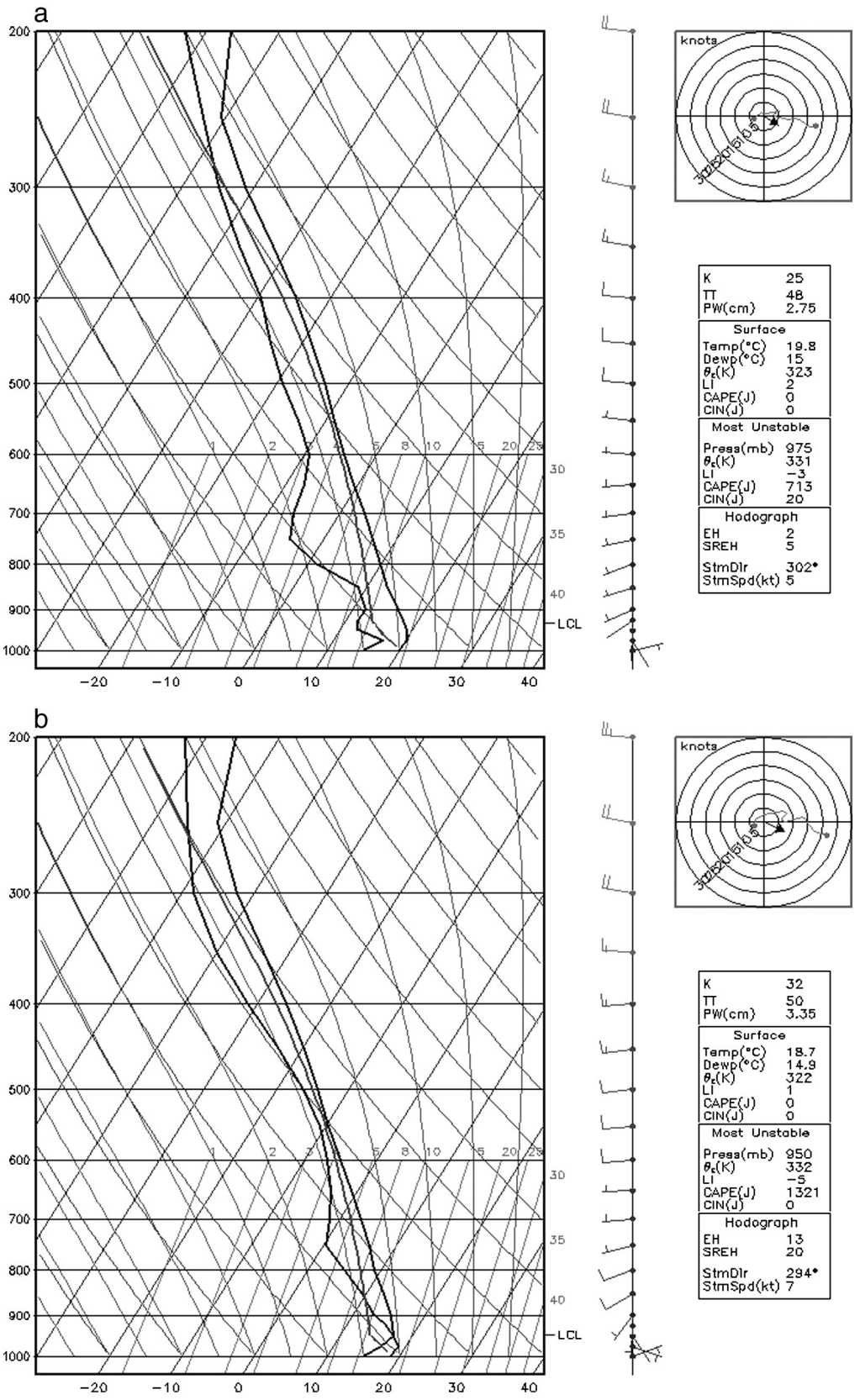

Fig. 9. a. WRF +12 h forecasted sounding at 46.0 N 13.0 E at 00 UTC, 12 September 2012. b. As in (a) but 6 h later (+18 h forecast).

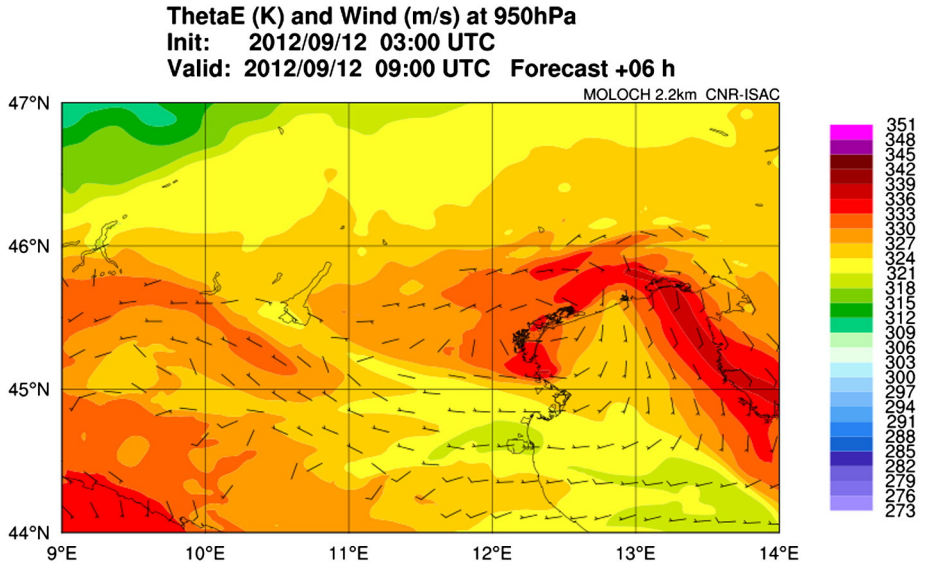

Fig. 10. Θ_e and wind at 950 hPa, forecast (+6 h) by MOLOCH at 0900 UTC.

see that the cold air flow moved faster and mainly over the sea in the WRF forecast, while it moved slower and mainly inland in the MOLOCH simulation. In this case, a multi-model approach would have been very effective, as the observed location of the squall-line lies right in between the forecast by the two models.

5. Cell propagation analysis

Further insights can be obtained by analyzing the propagation of storm centroids and also assessing the ability of the WRF model to forecast their trajectory. A particular emphasis is given to the morning (Rauscedo–Latisana–Grado) storms described in Section 3.2, characterized by the development of two cells moving along almost orthogonal paths. The solid lines of Fig. 13a show the cell centroid tracking, that has been identified by an algorithm based on the MODE tool of the MET verification software (Davis et al., 2009, see also http://www.dtcenter.org/met/users/docs/overview.php), developed by DTC–NCAR and here used for the meteorological analysis of the VMI radar field.

In correspondence with the development phase of the Northern cell (red solid line) the algorithm is not able to uniquely identify the centroid, resulting in an irregular path. After 0800 UTC the cell starts to move to the SE, when the Southern storm (blue line), just after initiation, slowly moves to the NE. At about 0830 UTC the two cells first meet near Latisana and, after that, a single (super)cell results from this interaction. The violet line, starting at 0910, tracks the new cell, that moves relatively slowly along a direction similar to that of the red line, reaching Grado just before 1100 UTC.

The dashed lines using a "▽" mark represent the propagation of the cell along a trajectory computed using the 850–300 hPa-layer mean wind, derived from the WRF hourly outputs (the end of the moving vector corresponds to the forecast shift one hour later). The dashed lines using a "+" mark are the trajectories based on the WRF surface-3 km-layer mean wind forecast. It is possible to see that only the blue cell moving from South of Concordia Sagittaria to Latisana follows this kind of trajectory.

After considering the mean wind displacements, two other specific tools have been tested. The first one is that proposed by Bunkers et al. (2000) for forecasting the movement of supercells. Their right-moving supercell motion vector is shown with a □ mark. Lastly, the Corfidi mesoscale convective system propagation vectors (Corfidi, 1998, 2003) have been computed. The dashed lines using a "x" mark indicates the "Corfidi downwind" propagation trajectories, while the "○" marks are the "Corfidi upwind" propagation vectors (details in Fig. 8 of Corfidi, 2003).

In particular, it can be noticed that between 0800 and 0900 UTC the Bunkers motion vector predicts the real motion of the Northern storm center much better than all the other techniques, showing a displacement coherent with the mesocyclonic supercell theory (Bunkers et al., 2000, and references therein). These results, together with the mesocyclone signature shown in Fig. 6a, b and c, support the classification of the Northern storm as a supercell. Note also that the path of the Northern cell deviates on the right side of about 75° with respect to the 850–300 hPa mean wind (▽ segment). The Southern storm approximately follows the 0–3 km mean wind propagation, possibly because this storm is still in a developing phase, even if VMI above 50 dBZ is already observed at 0800 UTC, reaching altitudes as high as 8 km (not shown). Lastly, the "merged" storm again follows more the Corfidi "upwind" direction, even if with a much shorter displacement (the violet path is 2 h long, while the motion vectors are forecasted for only 1 h). The Bunkers motion predicts a displacement that is slightly too much on the right side of the observed one, which deviates of only 40° with respect to the 850–300 hPa mean wind (▽ segment). According to the WRF simulation, the evolution of the storm after 0910 UTC could have been determined by the displacement of the cell into an area with higher low level winds, which

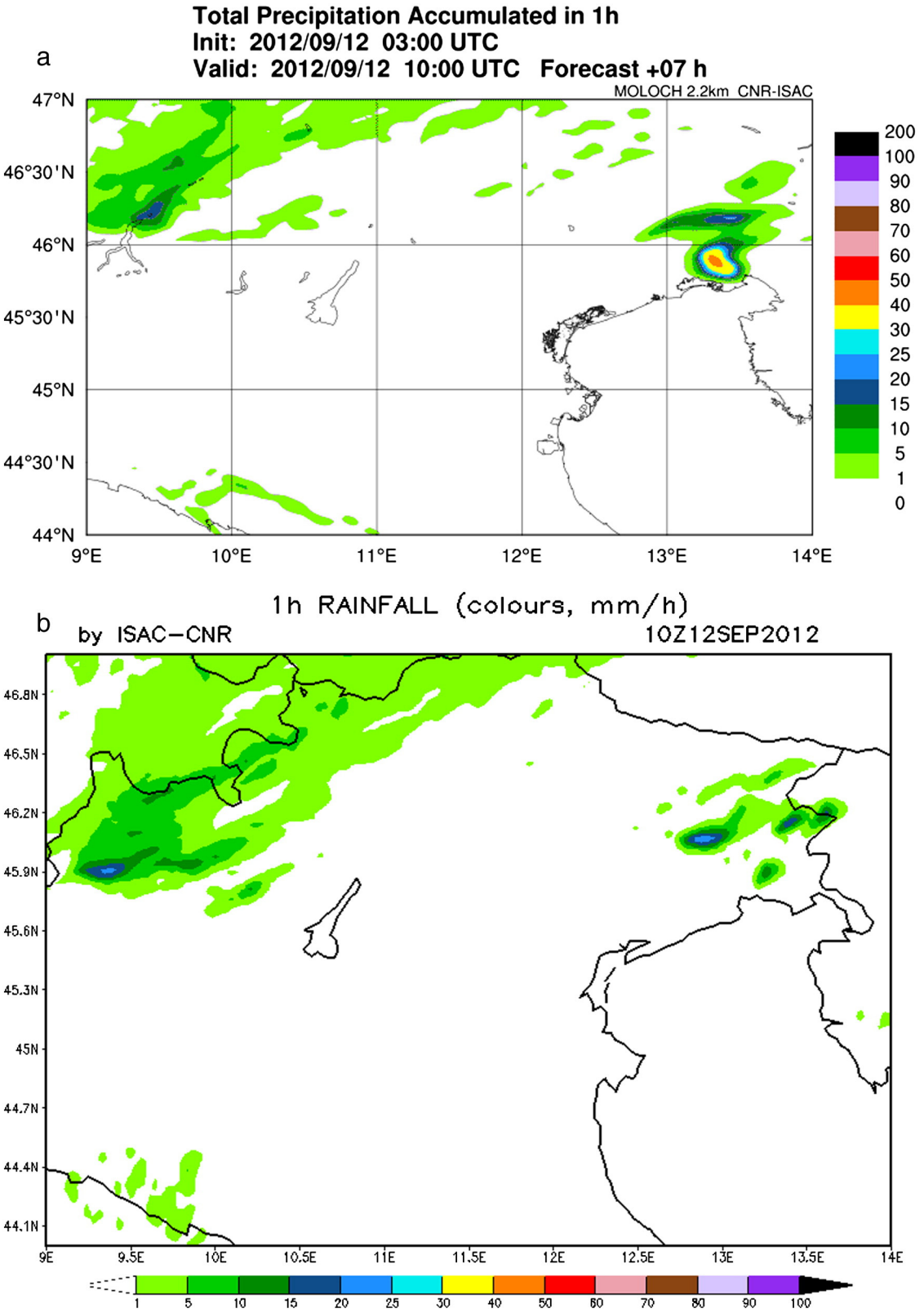

Fig. 11. a. Hourly accumulated precipitation forecast at 10 UTC, 12 September 2012 by MOLOCH (+7 h forecast). b. As in (a) but for WRF +22 h forecast (initialized at 1200 UTC of 11 September 2012).

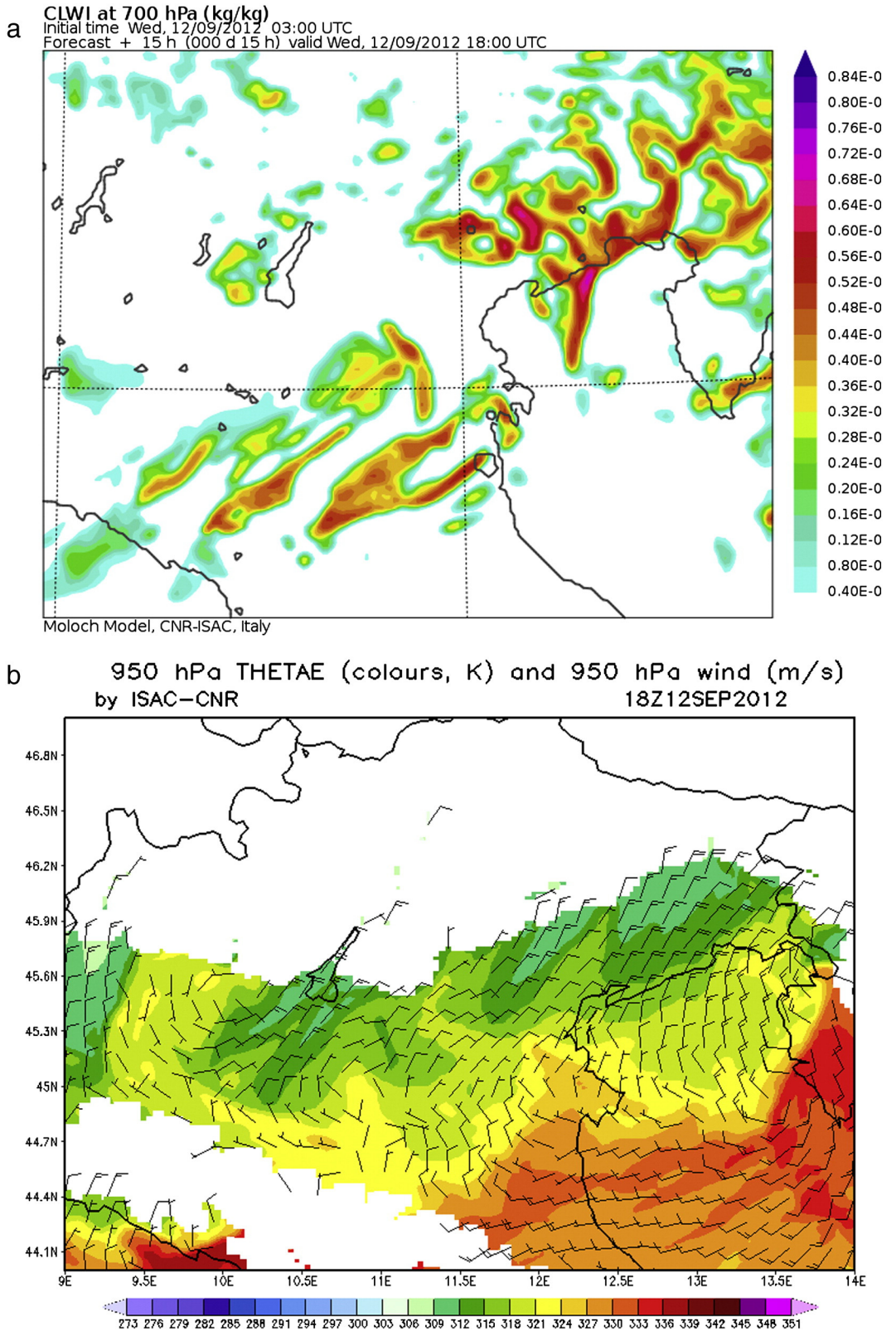

Fig. 12. Total cloud water and ice at 700 hPa (a) forecast by MOLOCH at 1800 UTC, 12 September 2012 (+15 h). Θ_e and wind at 950 hPa (b) forecast by WRF at 1800 UTC, 12 September 2012 (+30 h).

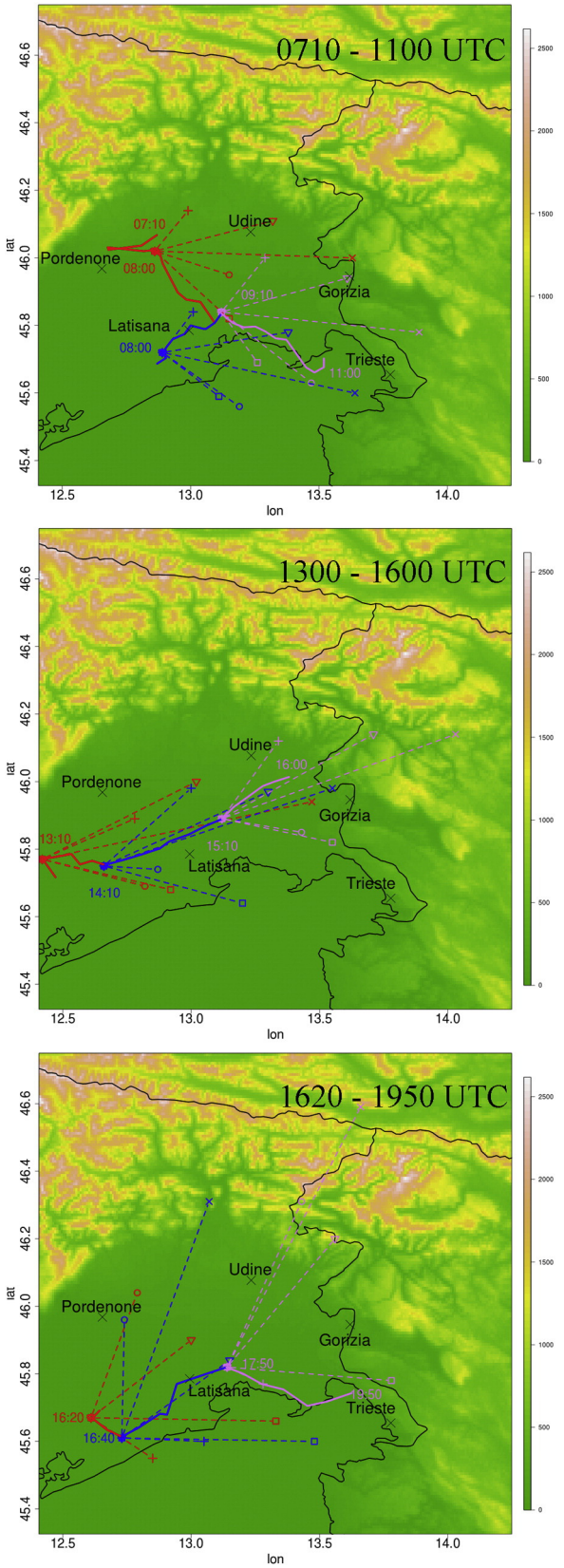

are an important element in the upwind Corfidi propagation mode theory.

Fig. 13b shows the propagation analysis of the early afternoon storm, between 1300 and 1600 UTC. The track can be divided into three phases, according to two abrupt changes in the storm propagation direction. During the first stage (red) the cell centroid path follows a direction parallel to the Corfidi upwind or the similar Bunkers forecasts (○ or □ segments), while, after 1410 UTC, it follows the Corfidi downwind (blue × segments) or the very similar mean 850–300 hPa-layer wind propagation trajectories (▽ segments). During the dissipation stage (violet segment), the propagation lies between the two mean-wind based trajectories (▽ 850–300 hPa mean wind or + sfc-3 km mean wind).

Finally, Fig. 13c shows the propagation of the storm, consisting in a developing organized line of several cells, during the late afternoon between 1620 and 1900 UTC. Here only the biggest centroid is analyzed. In the first stage (red color) the cell follows quite well the sfc-3 km mean wind, whereas in the middle (blue) phase the system follows well the mean 850–300 hPa wind (▽ segments), returning to the former propagation vector during the last stage (violet + segments), with the Bunkers segment being the second closest. In this case, no Corfidi propagation seems to describe any of the observed trajectories.

A final consideration can be drawn from the previous analysis: different phases of the storm life cycle correspond to different internal dynamics. The initial and final stages in general seem to be better described by the sfc-3 km mean wind (+). On the other hand, the intermediate stage is alternately described better by different techniques investigated here: in particular by Corfidi "upwind" direction for the 0910–1100 UTC storm and by the 850–300 hPa-layer mean wind for the two afternoon events. Particularly interesting is the forecast of the Northern supercell trajectory based on the Bunkers propagation vectors from 0800 to 0900 UTC, that seem to be well determined by the internal dynamics of a mesocyclonic supercell. Further refinements could be done on more cases, including, for example, information about maximum VMI, extension of the cell and storm life stage.

6. Results and conclusions

On 12 September 2012 different severe convective systems were observed over NEI. We focus particularly on the initial phase of the whole episode, between 0800–1100 UTC, characterized by the development of a supercell in the area within Rauscedo–Latisana–Grado. Two convective storms produced heavy precipitation up to more than 50 mm in 1 h (in the stations of San Vito and Palazzolo) and medium-sized hail (at least near Latisana). Coastal stations observed high value of low level Θ_e up to 342 K, also due to the + 1.5 °C anomaly of the

Fig. 13. Cell-centroid tracking (solid line) and WRF-based forecast using the mean sfc-3 km wind (+), mean 850–300 hPa wind (▽), Corfidi downwind propagation trajectory (×), Corfidi upwind propagation trajectory (○) and Bunkers vector (□), respectively for: the morning "Rauscedo–Latisana–Grado" case, "Mortegliano" afternoon case and "Grado" evening case.

northern Adriatic Sea SST, and Udine soundings highlighted strong potential instability for the period (DT500 of −5 °C).

The rapid scanning images, provided every 2.5 min for this event, proved to be critical for the identification of the relevant features during the evolution of the two systems at very short time scale, confirming the hypothesis that one system grew at the expense of the second one. In particular, an almost stationary low level convergence line above the northern Adriatic Sea played a major role in sustaining the deep convection inland. Between 0800 and 0845 UTC it was able to organize the preexisting convection in the Northern storm. Then, after the Southern storm intercepted the Northern one and its southerly inflow, the convergence line, pushed eastward by the strong winds associated to a mesoscale front, was able to change the internal dynamics of the resulting cell from supercell to a bow-echo-like storm.

The analysis of observations and model simulations agrees in identifying some factors responsible for the initiation of convection, in particular the convergence of a LLJ from the Adriatic with southwesterly Apennines foehn and with the barrier flow ahead of the Alps, generated by deflection of the LLJ itself in front of the orography. In addition, the triggering and the intensification of convective cells seem well related to the presence of this southerly moist low level jet. Such convergence seems to have been enhanced by the interaction with a cold front associated to the presence of a shallow mesoscale low over the Venice lagoon, well reproduced by the LAM simulations.

Although WRF and MOLOCH forecasts are affected by uncertainties on the exact timing and position of the storms and the intensity of associated rainfall, they are able to reproduce properly the mesoscale features (like the meso-low above Venice and the related cold front interacting with the convergence line) responsible for the development of the convective systems. Both models provide a clear signal of possible intense convective systems over the area in the morning, that could have helped the forecaster to identify dangerous situations, in particular in the presence of SST positive anomalies of the Adriatic Sea.

Later on, during the early afternoon, scattered and less predictable (due to the absence of large scale forcing) convection produced at least another intense storm, missed by the model forecasts, but well documented by the available observed data. Also this storm exhibited some supercell features, so that 12 September 2012 can be considered a supercell outbreak case in this region. The event terminated with the arrival of cold air overtaking the Alps, responsible for the formation of an organized convective system, resembling a small squall-line-like storm, whose effects and timing have been captured reasonably well by mesoscale models.

Finally, an analysis of the cell centroid propagation has been performed. It indicates that the initial and final stages tend to follow the sfc-3 km mean wind, while the most mature and intense stage seem to follow the 850–300 hPa mean wind or the Corfidi upwind propagation trajectory. Moreover, the morning supercell trajectory was well predicted by the Bunkers propagation vector. This result suggests that the mature stage of strong convection in this area could be identified also by a storm propagation that differs substantially from the sfc-3 km mean wind, but more cases should be analyzed to confirm this hypothesis.

Acknowledgments

Thanks to ARPAV, in particular to Dr. M. Ferrario, for providing data and images for Veneto region, to Mirko Bertato (OSMER — ARPA FVG) for providing HVMI and LBM radar images and to Marco Gani (OSMER — ARPA FVG) for editing the panel figures. We thank Dr John Mecikalski (The National Space Science & Technology Center, Alabama Univ.) for his suggestions and English improvement. This work is a contribution to the HyMeX program. The authors thank the whole Italian group involved in the SOP1 for the fruitful discussions and sharing of data. This study has been partly supported by the Italian flagship Project RITMARE, programme of CNR.

References

Atkins, N.T., St. Laurent, M., 2009. Bow Echo Mesovortices. Part II: their genesis. Mon. Weather Rev. 137, 1514–1532.

Barbi, A., Monai, M., Racca, R., Rossa, A.M., 2012. Recurring features of extreme autumnall rainfall events on the Veneto coastal area. Nat. Hazards Earth Syst. Sci. 12, 2463–2477.

Billet, S., Toro, E.F., 1997. On WAF-type schemes for multidimensional hyperbolic conservation laws. J. Comput. Phys. 130, 1–24.

Borga, M., Boscolo, P., Zanon, F., Sangati, M., 2007. Hydrometeorological analysis of the 29 August 2003 flash flood in the Eastern Italian Alps. J. Hydrometeorol. 8, 1049–1067.

Bunkers, M.J., Klimowski, B.A., Zeitler, J.W., Thompson, R.L., Weisman, M.L., 2000. Predicting supercell motion using a new hodograph technique. Weather Forecast. 15, 61–79.

Cacciamani, C., Battaglia, F., Patruno, P., Pomi, L., Selvini, A., Tibaldi, S., 1995. A climatological study of thunderstorm activity in the Po Valley. Theor. Appl. Climatol. 50, 185–203.

Corfidi, S.F., 1998. Forecasting MCS mode and motion. Preprints 19th conference severe local storms (Minneapolis, MN).

Corfidi, S.F., 2003. Cold pools and MCS propagation: forecasting the motion of downwind-developing MCSs. Weather Forecast. 18, 997–1017.

Davis, C.A., Brown, B.G., Bullock, R., Halley-Gotway, J., 2009. The Method for Object-Based Diagnostic Evaluation (MODE) applied to numerical forecasts from the 2005 NSSL/SPC Spring Program. Weather Forecast. 24, 1252–1267.

Davolio, S., Mastrangelo, D., Miglietta, M.M., Drofa, O., Buzzi, A., Malguzzi, P., 2009. High resolution simulations of a flash flood near Venice. Nat. Hazards Earth Syst. Sci. 9, 1671–1678.

Drofa, O.V., Malguzzi, P., 2004. Parameterization of microphysical processes in a non hydrostatic prediction model. Proc. 14th Intern. Conf. on Clouds and Precipitation (ICCP), Bologna, 19–23 July 2004, pp. 1297–3000.

Ducrocq, V., Braud, I., Davolio, S., Ferretti, R., Flamant, C., Jansa, A., Kalthoff, N., Richard, E., Taupier-Letage, I., Ayral, P.-A., Belamari, S., Berne, A., Borga, M., Boudevillain, B., Bock, O., Boichard, J.-L., Bouin, M.-N., Bousquet, O., Bouvier, C., Chiggiato, J., Cimini, D., Corsmeier, U., Coppola, L., Cocquerez, P., Defer, E., Drobinski, P., Dufournet, Y., Fourrié, N., Gourley, J.J., Labatut, L., Lambert, D., Le Coz, J., Marzano, F.S., Molinié, G., Montani, A., Nord, G., Nuret, M., Ramage, K., Rison, B., Roussot, O., Said, F., Schwarzenboeck, A., Testor, P., Van Baelen, J., Vincendon, B., Aran, M., Tamayo, J., 2013. HyMeX-SOP1, the field campaign dedicated to heavy precipitation and flash flooding in the northwestern Mediterranean. Bull. Am. Meteorol. Soc. http://dx.doi.org/10.1175/BAMS-D-12-00244.1 (in press).

Dudhia, J., 1989. Numerical study of convection observed during the Winter Monsoon Experiment using a mesoscale two-dimensional model. J. Atmos. Sci. 46, 3077–3107.

Ferretti, R., Pichelli, E., Gentile, S., Maiello, I., Cimini, D., Davolio, S., Miglietta, M.M., Panegrossi, G., Baldini, L., Pasi, F., Marzano, F.S., Zinzi, A., Mariani, S., Casaioli, M., Bartolini, G., Loglisci, N., Montani, A., Marsigli, C., Manzato, A., Pucillo, A., Ferrario, M.E., Colaiuda, V., Rotunno, R., 2014. Overview of the first HyMeX special observation period over Italy: observations and model results. Hydrol. Earth Syst. Sci. 18, 1953–1977.

Feudale, L., Manzato, A., Micheletti, S., 2013. A cloud-to-ground lightning climatology for North Eastern Italy. Advances in Science and Research. 10,, pp. 77–84, (available online at http://dx.doi.org/10.5194/asr-10-77-2013).

Galway, J.G., 1956. The lifted index as a predictor of latent instability. Bull. Am. Meteorol. Soc. 37, 528–529.

Giaiotti, D., Nordio, S., Stel, F., 2003. The climatology of hail in the plain of Friuli–Venezia Giulia. Atmos. Res. 67–68, 247–259.

Isotta, F.A., Frei, C., Weilguni, V., Perčec Tadić, M., Lassègues, P., Rudolf, B., Pavan, V., Cacciamani, C., Antolini, G., Ratto, S.M., Munari, M., Micheletti, S., Bonati, V., Lussana, C., Ronchi, C., Panettieri, E., Marigo, G., Vertačnik, G., 2013. The

climate of daily precipitation in the Alps: development and analysis of a high-resolution grid dataset from pan-Alpine rain-gauge data. Int. J. Climatol. 34 (5), 1657–1675.

Janjic, Z.I., 2001. Nonsingular implementation of the Mellor–Yamada Level 2.5 Scheme in the NCEP Meso model. NCEP Tech. Rep. 437 (61 pp.).

Kain, J.S., 2004. The Kain–Fritsch convective parameterization: an update. J. Appl. Meteorol. 43, 170–181.

Kerkmann, J., Setvák, M., Manzato, A., 2012. Experimental 2.5-minute super rapid scans from MSG-3 capture a supercell storm above northern Italy (12 September 2012). EUMETSAT report (Available online at: http://oiswww.eumetsat.org/-WEBOPS/iotm/-iotm/20120912_convection/-20120912_convection.html).

Malguzzi, P., Grossi, G., Buzzi, A., Ranzi, R., Buizza, R., 2006. The 1966 'century' flood in Italy: a meteorological and hydrological revisitation. J. Geophys. Res. 111. http://dx.doi.org/10.1029/2006JD007111 (D24106).

Manzato, A., 2012. Hail in NE Italy: climatology and bivariate analysis with sounding-derived indices. J. Appl. Meteorol. Climatol. 51, 449–467. http://dx.doi.org/10.1175/JAMC-D-10-05012.1.

Manzato, A., Morgan, G.M., 2003. Evaluating the sounding instability with the Lifted Parcel Theory. Atmos. Res. 67–68, 455–473.

Mlawer, E.J., Taubman, S.J., Brown, P.D., Iacono, M.J., Clough, S.A., 1997. Radiative transfer for inhomogeneous atmosphere: RRTM, a validated correlated-k model for the longwave. J. Geophys. Res. 102, 16663–16682.

Morcrette, J.-J., Barker, H.W., Cole, J.N.S., Iacono, M.J., Pincus, R., 2008. Impact of a new radiation package, McRad, in the ECMWF Integrated Forecasting System. Mon. Weather Rev. 136, 4773–4798.

Morgan Jr., G.M., 1973. A general description of the hail problem in the Po Valley of Northern Italy. J. Appl. Meteorol. 12, 338–353.

Niu, G.-Y., Yang, Z.-L., Mitchell, K.E., Chen, F., Ek, M.B., Barlage, M., Longuevergne, L., Kumar, A., Manning, K., Niyogi, D., Rosero, E., Tewari, M., Xia, Y., 2011. The community Noah land surface model with multiparameterization options (Noah-MP): 1. Model description and evaluation with local-scale measurements. J. Geophys. Res. 116, D12. http://dx.doi.org/10.1029/2010JD015139.

Pucillo, A., Manzato, A., 2010. 08/08/08: the "Olympic storm" event and its implication about severe weather. Poster at IV Hymex Workshop, Bologna 8–10 June 2010 (page 71 in Book of Abstracts of IV Hymex Workshop, available online at: www.hymex.org/public/workshops/4/BOOK_OF_ABSTRACT_HYMEX_2010.pdf?1407740830).

Riesco Martin, J., Mora Garcia, M., de Pablo Davila, F., Rivas Soriano, L., 2013. Severe rainfall events over the western Mediterranean Sea: A case study. Atmospheric Research 127, 47–63.

Ritter, B., Geleyn, J.F., 1992. A comprehensive radiation scheme for numerical weather prediction models with potential applications in climate simulations. Mon. Weather Rev. 120, 303–325.

Setvák, M., Charvát, Z., Valachová, M., Bedka, K., 2012. Blended "sandwich" image products in nowcasting. Proc. 2012 EUMETSAT Meteorological Satellite Conference, Sopot, Poland (EUMETSAT P.61).

Skamarock, W.C., Klemp, J.B., Dudhia, J., Gill, D.O., Barker, D.M., Wang, W., Powers, J.G., 2005. A description of the advanced research WRF version 2. NCAR Technical Note 468STR (88 pp.).

Thompson, G., Rasmussen, R.M., Manning, K., 2004. Explicit forecasts of winter precipitation using an improved bulk microphysics scheme. Part I: description and sensitivity analysis. Mon. Weather Rev. 132, 519–542.

Zampieri, M., Malguzzi, P., Buzzi, A., 2005. Sensitivity of quantitative precipitation forecasts to boundary layer parameterization: a flash flood case study in the Western Mediterranean. Nat. Hazards Earth Syst. Sci. 5, 603–612.